RSC Advances


This is an *Accepted Manuscript*, which has been through the Royal Society of Chemistry peer review process and has been accepted for publication.

*Accepted Manuscripts* are published online shortly after acceptance, before technical editing, formatting and proof reading. Using this free service, authors can make their results available to the community, in citable form, before we publish the edited article. This *Accepted Manuscript* will be replaced by the edited, formatted and paginated article as soon as this is available.

You can find more information about *Accepted Manuscripts* in the Information for Authors.

Please note that technical editing may introduce minor changes to the text and/or graphics, which may alter content. The journal's standard Terms & Conditions and the Ethical guidelines still apply. In no event shall the Royal Society of Chemistry be held responsible for any errors or omissions in this *Accepted Manuscript* or any consequences arising from the use of any information it contains.

ROYAL SOCIETY OF CHEMISTRY

www.rsc.org/advances

# A facile method to prepare composite and porous polyphosphazene membranes and investigation to their properties

Lei Hu, Aiqing Zhang, Kai Liu, Shan Lei, Guangxin Ou, and Xinjian Cheng*

School of Chemistry and Materials Science, South-central University for Nationalities, Wuhan, P. R. China, 430074

Abstract: Polyphosphazene/$SiO_2$ composite membranes and porous polyphosphazene membranes were prepared and their properties were studied in detail. In this work, linear polyphosphazenes with 3-aminopropyltriethoxysilane (APTS) and n-butylamino side groups were prepared via the nucleophilic substitution reaction. The substituted polyphosphazenes were cross-linked by the hydrolysis of triethoxysilanes to form polyphosphazene/$SiO_2$ composite membranes. When the as-prepared polyphosphazene/$SiO_2$ composites were treated by HF, the silica dissolved and porous polyphosphazene membranes formed subsequently. Their structures and morphologies were studied by IR, DSA, DMA, XPS and SEM. And their mechanical properties were investigated as well. It could be seen that the thermal stability, the contact angles and the mechanical properties changed with the ratio of APTS. Namely, the contact angle changed from 74° to 96°, and the initial decomposition temperature increased from 170℃ to 225℃ when the ratio of APTS increased. Besides, the glass transition temperature increased from -48℃ to 31℃ after the membranes were cross-linked.

Keywords: composite membrane, porous membrane, contact angle, $T_g$

*Corresponding author: Dr. Cheng, chxj606@163.com.



RSC Advances Accepted Manuscript

## Introduction

Polyphosphazene finds wide applications due to the adjustable side groups on its backbone [1, 2]. This polymer is usually prepared through two-step reactions [3-5]. The first step is thermal ring-opening polymerization of hexachlorocyclotriphosphazene (HCTP) to obtain the macromolecules [5]. The second one is a nucleophilic substitution reaction by organic side groups, such as $–NH_2$ [6] and –ONa [7].

The special structure makes the backbone of polyphosphazene highly flexible that could be used as elastomers [8, 9]. Polyphosphazene is also well-known for its biomedical uses [10, 11]. The excellent biocompatibility and biodegradability of polyphosphazenes make them often used as biomaterials. The research on phosphazene biomaterials has achieved great progress in recent years [12, 13]. For example, Ren et al. [14] have successfully incorporated saccharide moieties into polyphosphazenes via thiol-yne click chemistry. The glycosylated polyphosphazene had a potential use for protein recognition and separation. Barrett et al. [15] studied a series of polyphosphazenes for the applications as “cell-compatible” substrates. Their works show that these polyphosphazenes could provide an efficient and cost-effective platform for patterned cell culture systems. Krogman et al. [16] have synthesized tris(hydroxymethyl)amino methane and alanine ethyl ester substituted polyphosphazenes. And they have also prepared polymer blends of these polymers and poly(lactide-co-glycolide) (PLGA). Their studies suggested that the blends have a

RSC Advances Accepted Manuscript

promising application to generate a porous structure with some residual strength for the different hydrolytic activities of the two polymers.

Silica is frequently used as biomaterials as well. It possesses excellent properties such as biocompatibility [17, 18], biodegradability [19, 20] and physicochemical stability [21-23]. Thereby studies of silica materials in the biomedical fields have attracted great attention [24, 25]. For example, He et al. [25] have reported highly ordered MCM-41-type mesoporous silica nanoparticles (MSNs) with particle sizes about 150nm. They prepared the silica materials by grafting PEGxk chains of different molecular weights and chain densities on the outer surface of the particles. The modified MSNs could be used in controllable drug delivery and used as bio-signal sensing materials.

In addition, silica could be used as reinforcing materials. Polymeric materials could be reinforced by the introduction of silica to polymer matrix. For example, Cheng et al [26] prepared an organophilic organic-inorganic composite urethane acrylate with silsesquioxane bearing terminal hydroxyl groups on the outermost Surface. In contrast to conventional UV-curable resins, the hybrid system is rather stable and the preparation is convenient. Better mechanical and physical properties are also observed owing to the synergism between organic and inorganic components.

In this work, silica and polyphosphazene were combined together to form a new membrane material which possess the merits of the two components. Polyphosphazene/$SiO_2$ composite membranes were synthesized by hydrolysis of aminopropyltriethoxysilane substituted polyphosphazene. The wettability, thermal



RSC Advances Accepted Manuscript

stability and mechanical properties of the as-prepared polyphasphozene membranes changed with the reaction conditions. Furthermore, porous polyphosphazenes were prepared by treating the polyphosphazene/$SiO_2$ composite membranes with HF. Both the composite and porous polyphosphazene membranes have a great prospect in medical application, tissue engineering and membrane technology.

## 1. Experimental section

### 1.1 materials

Tetrahydrofuran (THF), n-hexane, calcium hydride ($CaH_2$), petroleum ether (PE), n-butylamine, triethylamine (TEA), sodium, ammonium hydroxide (25% $NH_3$) and Hydrofluoric acid (40% HF, aqueous solution) were purchased from Sinopharm Chemical Reagent Co. Hexachlorocyclotriphosphazene (HCTP) was purchased from Aladdin Chemical Co. Ltd. It was purified by re-crystallization from n-hexane and subsequent vacuum sublimation at 60°C. 3-Aminopropyltriethoxysilane (APTS) was purchased from J&K China Chemical Ltd. Reagents and solvents were used as received without further treatment unless stated.

### 2.2 Characterizations

$^1H$ NMR and $^{31}P$ NHR spectra were collected on Bruker AVANCE Ⅲ 400 MHz Digital NMR spectrometer in $d_6$-$CDCl_3$ using TMS and 85% $H_3PO_4$ as internal standards. Fourier transform infrared (FT-IR) spectra were obtained on a Nicolet NEXUS 470 spectrometer. X-ray photoelectron spectroscopy analysis was carried on a spectrometer (Thermo VG Multilab 2000) using an Al Ka X-ray source (300 W PE 25 eV). Thermo gravimetric analysis (TGA) measurements were recorded on



RSC Advances Accepted Manuscript

NETZSCH TG 209F3 apparatus at a heating rate of 10℃/min under $N_2$ atmosphere. The dried samples were heated from 40 to 800℃. The contact angle of water was measured by Drop Shape Analysis System (KRÜSS GmbH, DSA100). The mechanical properties were tested on Tensile Testing Machine WSM-20KN (Changchun INTELLIGENT APPARATUS CO., LTD) at a shift rate of 1mm/min. The micrographs of fractured cross-section of the membranes were obtained via field emission scanning electron microscopy (JEOL JSM-7600F) under the accelerating voltage of 15.0kv. Dynamic mechanical analysis was conducted on a DMA Q800, TA instrument, from -100℃ to 70℃, 10℃/min. The specific surface areas of porous membranes were obtained using BET model for adsorption data in a relative pressure ranged from 0.05 to 0.30 on Quantachrome Autosorb-1-C-MS spectra. Before BET testing, each sample was degassed at 80℃ for 6h.

**2.3 Preparation of polyphosphazene membranes**

**2.3.1 Preparation of poly[di(chloro)phosphazene]**

The poly[di(chloro)phosphazene] (PDCP) was prepared using the method described in our previous work [27].

**2.3.2 Preparation of Poly[di(3-Aminopropyltriethoxysilane)phosphazene](PDA)**

PDCP (4.636g, 0.04mol) was dissolved in 200ml dry THF in a three-neck flask equipped with a dropping funnel, an argon purge and a refluxing condenser. APTS (18.595g, 0.084mol) and TEA (4.501g, 0.084mol) in 100ml THF were added dropwise within 30min. The mixture was stirred at room temperature for 48 h, and heated to reflux for 24 hours to obtain PDA. Afterwards, the mixture was vacuum



RSC Advances Accepted Manuscript

filtered for three times in a glove box to remove the insoluble salts. And then THF was pumped out at room temperature to get the yellowish products. To purify the product, the yellowish products were re-dissolved in 50ml THF and then precipitated in PE twice. Finally, the resultant PDA was dried under a vacuum at 40℃ for 24h to yield 14.278g (73.5%).

**2.3.3 Preparation of Poly[(APTS)$_x$/(butylamino)$_y$phosphazene] (PAB)**

PAB could be synthesized using the same equipment and method mentioned above. A typical recipe was described as follows: PDCP (4.636g, 0.04mol) was dissolved in 200ml THF. After that, THF (50ml), APTS (8.855g, 0.04mol) and TEA (4.250g, 0.042mol) were added dropwise in about 30min and stirred for 12h. Butylamine (3.072g, 0.042mol) and TEA (4.250g, 0.042mol) in 50ml THF were injected into the dropping funnel and added dropwise in 30min. The mixture was stirred at room temperature for another 12 hours, and heated to reflux for 24 hours. Afterwards, the mixture was vacuum filtered for three times in glove box to remove the insoluble salts. And then THF was pumped out to get the yellowish products. The resultant polymer was named PAB50 in this paper for the ratio of substituted APTS accounting for 50% of the total substituent groups. By changing the ratio of allylamino and n-butylamino, PAB1 with substituted APTS of 1% of total substituent groups, PAB5 with substituted APTS of 5% of total substituent groups, PAB20 with substituted APTS of 20% of total substituent groups were synthesized via the same method.

**2.3.4 Preparation of cross-linked polymer membranes from PDA and PAB**



RSC Advances Accepted Manuscript

A solution was obtained by dissolving PDA or PAB of varying substituent-degree in THF and poured into a polytetrafluoroethylene (PTFE) slot and covered by a glass beaker to slow down the THF evaporation. After about 48h, yellowish membranes were obtained and put into an iron dish within ammonium hydroxide (25% $NH_3$) overnight. And then, the membranes were washed by deionized water and dried in vacuum at 40℃ overnight. Through the hydrolysis and condensation of APTS, the polyphosphazenes were cross-linked.

**2.3.5 Preparation of porous polyphosphazene membranes**

The cross-linked PDA and PABs were soaked in 10% hydrofluoric acid for 2h to ensure that all the $SiO_2$ could be destroyed completely. Afterwards, the HF etched membranes were washed by deionized water and dried in vacuum under 40℃ overnight. The porous polyphosphazene membrane was obtained accordingly.

RSC Advances Accepted Manuscript

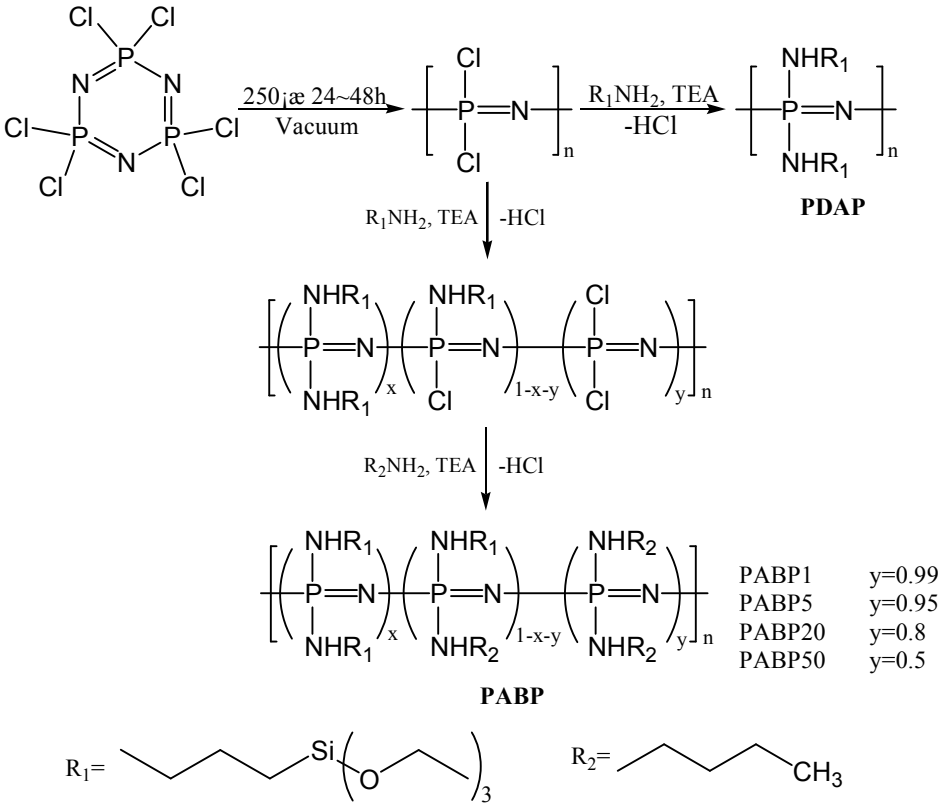


Figure 1 Synthesis route of linear polyphosphazenes

## 2.4 Measurement of swelling degree

The measurement of swelling degree was done according to the literature [27]. A series of cross-linked polyphosphazene membranes were soaked in THF for 24h. Then THF was poured out carefully and the unabsorbed solvent on the membrane was sucked by filter paper. Afterwards, the swollen membrane was weighed. The awelling degree was calculated using the following equation:

$$\text{Swelling Degree [ \% gg}^{-1}\text{ ]} = \frac{M_1 - M_0}{M_0} \text{ ¡Á100} \quad (1)$$

Wherein $M_0$ stands for the weight of dry membranes, $M_1$ stands for the mass of the swollen polymer films.

## 3 Results and Discussion



RSC Advances Accepted Manuscript

### 3.1 Preparation of the linear and cross-linked polyphosphazenes membranes

The functional groups in this work, 3-aminopropyltriethoxysilane, were used to substitute Cl atoms on the chains of PDCP by nucleophilic substitution reaction with TEA as acid-binding agent. In order to get varying replacing-degree of 3-aminopropyltriethoxysilane, n-butylamino was introduced as an inert substituent. The synthetic route is shown in Fig.1. And the parameters of replacement reactions are summarized and shown in Tab. 1.

Table 1 The parameters of replacement reaction

| **Products** | **PDCP (g/mmol)** | **APTS/TEA[a] (g, mmol/g, mmol)** | **n-Butylamine/TEA[b] (g, mmol/g, mmol)** | **Yield (g/%)** | **Solvent** |
|---|---|---|---|---|---|
| **PAB1** | 4.636/40 | 0.186, 0.8/0.085, 0.84 | 6.144, 84/8.50, 84 | 5.549/72.2 | THF/EtOH |
| **PAB5** | 4.636/40 | 0.930, 4.2/0.425, 4.2 | 5.837, 79.8/8.076, 79.8 | 5.834/71.5 | THF/EtOH |
| **PAB20** | 4.636/40 | 3.719, 16.8/1.7, 16.8 | 4.915, 67.2/3.400, 6.8 | 7.643/76.9 | THF/EtOH |
| **PAB50** | 4.636/40 | 8.855, 42/4.250, 42 | 3.072, 42/4.250, 42 | 10.257/76.0 | THF/EtOH |
| **PDA** | 4.636/40 | 18.595, 84/8.501, 84 | - | 14.278/73.5 | THF/EtOH |

(a) Reacted at RT for 12h and injected b.

(b) Reacted at RT for 12h and heated to reflux for 24h.

All the linear substituted polyphosphanzenes were characterized by $^{31}$P-NMR and $^{1}$H-NMR. For protection from the hydrolysis in the air, the linear polyphosphazenes were kept in glove box and the $d_6$-$CDCl_3$ was dried by $CaH_2$ before use.

The $^{1}$HNMR and $^{31}$P NMR of PDA and PAB were carried out in Fig. 2 and Fig.3. Fig 2a is the $^{31}$P NMR spectra of PDA; Fig 2b is $^{1}$HNMR spectra of PDA. Fig 3



RSC Advances Accepted Manuscript

showed a typical PAB sample, PAB20. The mole ratio of APTS/BA grafting on PAB was computed from $^{1}$H-NMR data by comparing the peak intensities of methylene protons of ethyoxyl at $\delta$ =3.83 to the methyl protons of BA at $\delta$ =0.93.

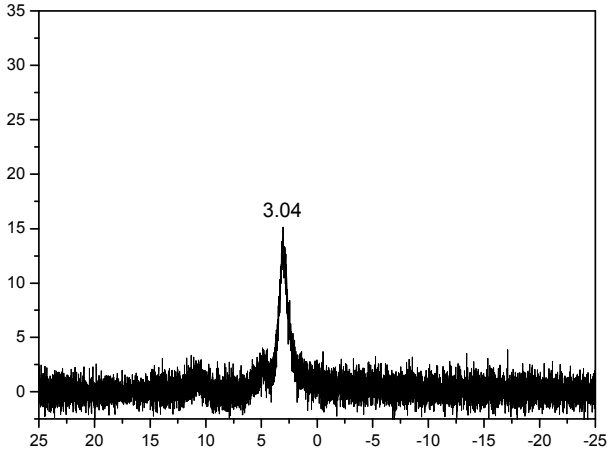


Figure 2a $^{31}$P-NMR of PDA

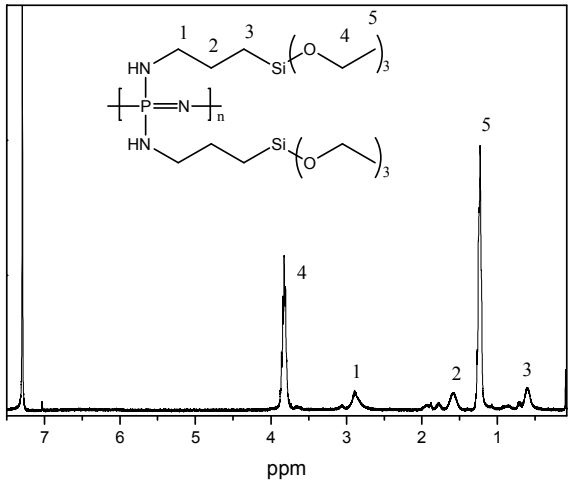


Figure 2b $^{1}$H-NMR of PDA

RSC Advances Accepted Manuscript

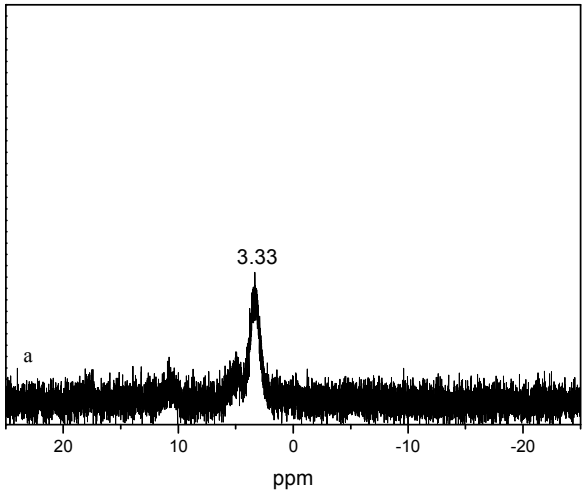


Figure 3a $^{31}$P-NMR of PAB20

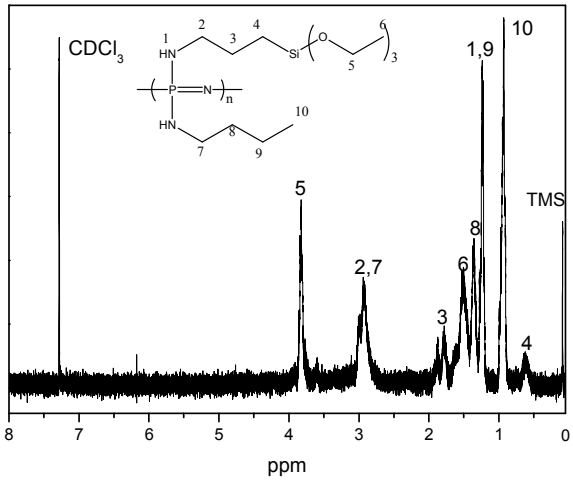


Figure 3b $^{1}$H-NMR of PAB20

The cross-linked polyphosphazenes were characterized by FTIR. As showed in Fig. 4 (FTIR spectroscopy of PAB50), the strong and broad absorbance at about 3300cm$^{-1}$ corresponds to stretching vibration of N–H. And the peak at 3411cm$^{-1}$ corresponds to the stretching vibration of Si-O. The peaks of 2970cm$^{-1}$, 2930cm$^{-1}$ and 2834cm$^{-1}$ correspond to the absorbance of –$CH_2$– and –$CH_3$. The peaks at 1101cm$^{-1}$ and



RSC Advances Accepted Manuscript

954cm$^{-1}$ correspond to the skeleton vibration of polyphosphazene and P–N–C. Furthermore, the peak at about 1100cm$^{-1}$ also corresponds to the silica segments. The peaks at 1248cm$^{-1}$ and 774cm$^{-1}$ correspond to the absorbance of Si-C and Si-O respectively. The strong absorption of P–Cl from 540 to 580cm$^{-1}$ becomes very weak here and even disappears. The data of NMR and IR is consistent with prospection of the structure of PDA and PAB and suggests that the chlorine in PDCP was replaced completely.

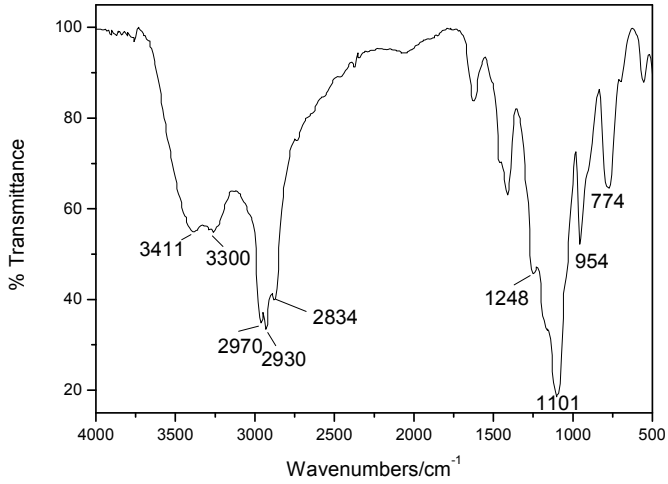


Figure 4 FTIR of cross-linked PAB50

### 3.2 Propeties of polyphosphazenes

#### 3.2.1 Surface wettability

The surface wettability of material was characterized from the data of contact angles (CA). All the cross-linked polymer membranes were flat on a plain glass sheet and its contact angles (CA) of deionized water were measured by DSA. As the Fig. 5 shows, the ratio of APTS has an influence on the CA. As we know, the backbone of the polyphosphazene is hydrophilic [1] while silica segment is more hydrophobic. The



RSC Advances Accepted Manuscript

CA data indicated that the increasing silica segment may result in the increasing of CA. Detailed data are showed in table 2.

Table 2 Wettability and mechanical properties

| Products | CA[a]/° | EB[b] | TS[c]/MPa |
|---|---|---|---|
| PAB1 | 74 | 1.04 | 1.84 |
| PAB5 | 82 | 0.43 | 2.03 |
| PAB20 | 85 | 0.13 | 2.12 |
| PAB50 | 92 | 0.11 | 2.31 |
| PDA | 96 | 0.06 | 1.93 |

(a) Cross-linked polyphosphazenes, (b) Elongation at break, (c) Tensile strength.

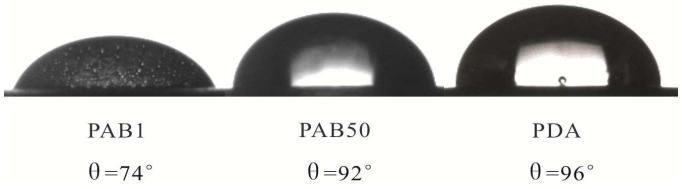


Figure 5 Photos of the Contact angle of cross-linked polyphosphazenes

### 3.2.2 Thermal decompose temperature

The initial decomposition temperatures ($T_i$) of cross-linked polyphosphazenes were carried out by thermogravimetric analysis (TGA). Comparing PAB1 ($T_i$=170℃) and PDA ($T_i$=225℃) in Fig. 6, it was revealed that the higher of the ratio of APTS, the better of thermal stability. It resulted in that the thermal stability enhanced with the increasing of ratio of APTS. Moreover, the thermal stability of polymers could be also enhanced by the incorporation of silica. The amount of silica in composite membranes increased with the ratio of APTS. The residues above 600 $^{o}$C might be come from



RSC Advances Accepted Manuscript

silica. Overall, all the cross-linked polyphosphazenes will not decomposed until 170℃, and the $T_i$ of PDA could reach 225℃.

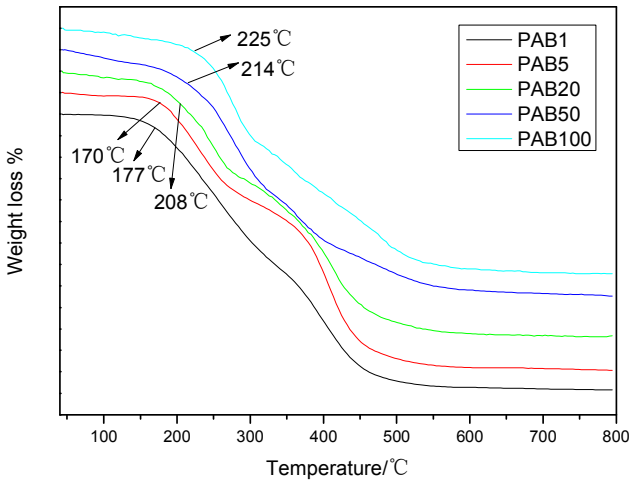


Figure 6 TGA of the cross-linked polyphosphazenes

### 3.2.3 Dynamic Mechanical Analysis (DMA)

All the data of DMA testing was shown in Fig 7 and Fig 8. Fig 7 showed the storage modulus *vs* the temperature. It could be seen in Fig7, from about -50℃ to room temperature, the storage modulus of PAB50 which was untreated by $NH_3 \cdot H_2O$ remains low compared to the cross-linked polymers. Under the same temperature, the higher of the ratio of APTS, the higher of the storage modulus.

RSC Advances Accepted Manuscript

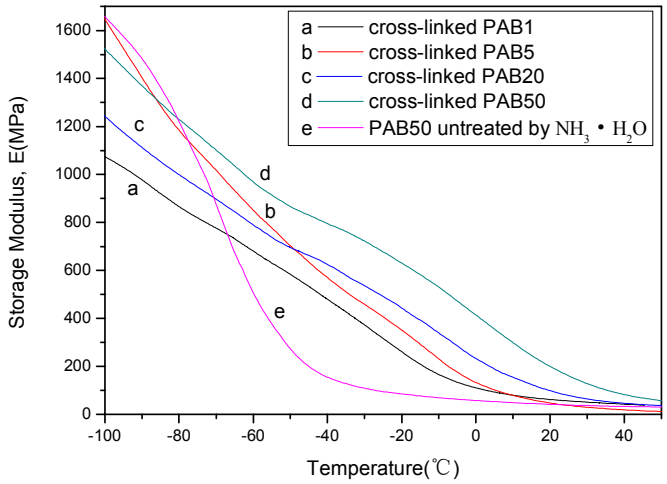


Figure 7 Dynamic mechanical measurements of the storage modulus

In Fig. 8, the Tan δ *vs* temperature was plotted. The $T_g$ of the samples could be find at the peak of each curve. It could be found that the uncross-linked sample showed the lowest $T_g$ of -48 ℃(curve e). However, when the membranes were cross-linked, the $T_g$ increased with the ratio of APTS, from -11℃ to 31℃. Moreover, the stress-strain curves were illustrated in Fig. 9. It could be seen clearly that when the amount of APTS increased, the composite membrane became relatively rigid, though all of them are elastomers.

RSC Advances Accepted Manuscript

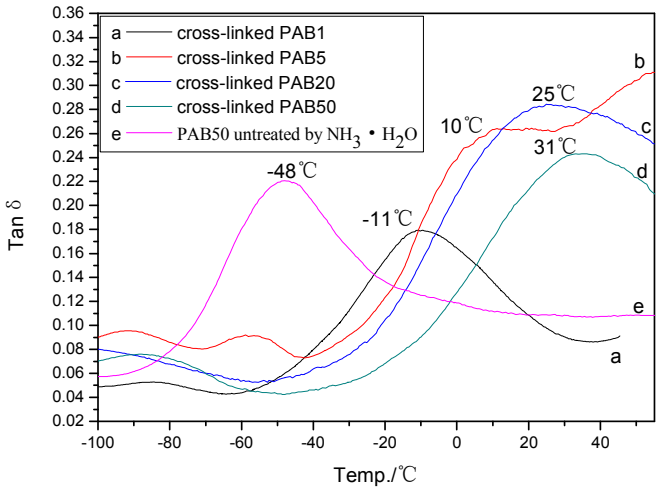


Figure 8 Dynamic mechanical measurement of Tan δ

### 3.2.4 Mechanical properties

The Elongation at breaking (EB) and Tensile strength (TS) of cross-linking membranes were tested. As is showed in Tab. 2, the EB decreased from 1.043 to 0.055 as the substitution degree increased. Furthermore, comparing the EB of PAB1 and PAB5, PAB5 and PAB20, the rate of increasing of EB tended to slowdown. It reveals that the downward trend of the EB get to slow as the cross-linking density increase. Moreover, the TS also presented some regularity along with the substitution degree. As the substitution increased, the TS increased but the TS of the PDA (1.931MPa) are an exception even lower than PAB5. Figure 9 shows the typical stress-strain curves.

RSC Advances Accepted Manuscript

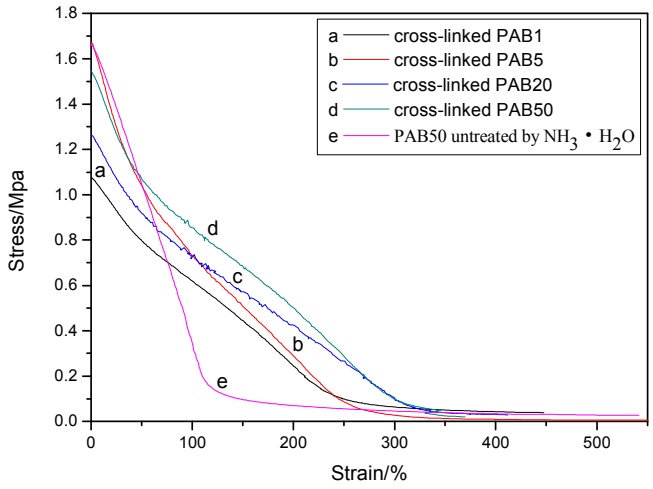


Figure 9 Representative stress-strain curves

### 3.2.5 XPS measurement

PDCP, cross-linked PAB20 and the etched PAB20 were tested by XPS respectively, and the result is showed in Fig. 10. Comparing curve a and curve b, the peak of Cl 2p disappeared in curve b while the peak of Si 2p raised. It indicated that Cl on the backbone of the PDCP was substituted by 3-Aminopropyltriethoxysilane and n-butylamino completely. Comparing curve c and curve b, the peak of F 1s in curve c illustrated that the silica segment was etched by HF and the Si-F was formed. The peaks of C 1s and O 1s in curve a may resulted in the effect of moist air on PDCP. Overall, the XPS analysis provided more evidences that the PDCP could be substituted completely and the cross-linked polyphosphazenes could be etched successively to form porous polyphosphazene membranes.

RSC Advances Accepted Manuscript

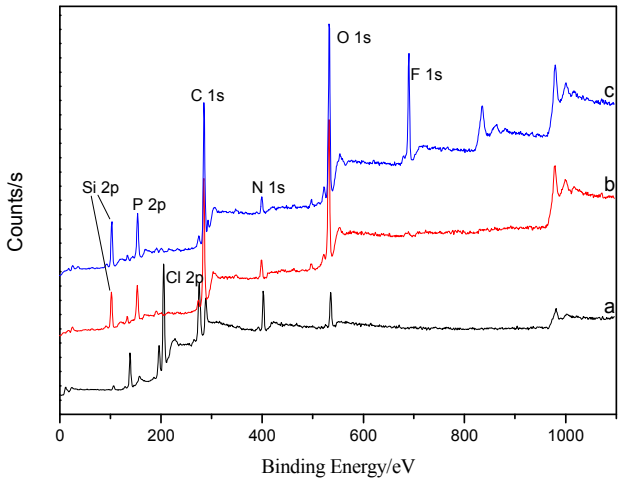


Figure 10 XPS of polyphosphazenes

(a) PDCP, (b) Cross-linked PAB20, (c) Cross-linked PAB20 soaked in HF for 2h.

### 3.2.6 Swelling behavior

All the swelling degree data of cross-linked composite polyphosphazene membranes were illustrated in Fig. 11. It could be seen that the ratio of APTS has a great effect on swelling behavior. It could be deduced from the data of PAB1 and PDA that the higher of the ratio of APTS, the lower of the swelling degree. However, the downward trend of the swelling degree got to slow when the ratio of APTS reached a certain value.

RSC Advances Accepted Manuscript

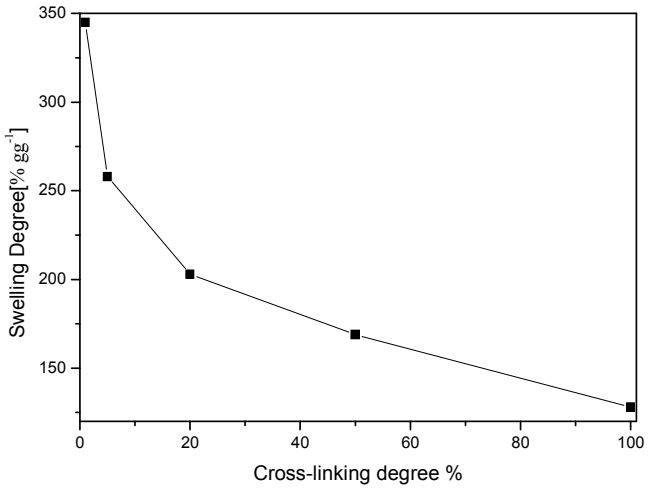


Figure 11 Relation of ratio of APTS and Swelling degree of hybrid membranes in THF at RT

### 3.2.7 Specific surface area (SSA)

For proving the porous structure of etched polyphosphazenes, the surface area was studied via BET method. The samples of polyphosphazenes etched by HF were degassed at 80℃ before testing and analyzed using Brunauer-Emmett-Teller (BET) model for adsorption data under a relative pressure from 0.05 to 0.30. Fig. 12 clearly illustrated that SSA increased with the ratio of APTS. When 5% APTS was used, the **SSA** was $0.27X10^{-1}$ $m^2/g$; and when 100% APTS was used, the SSA increased to 4.2 $X10^{-1}$ $m^2/g$. It indicated that the APTS used, the more silica particles formed. The more pores could be obtained when the silica particles were etched by HF.

RSC Advances Accepted Manuscript

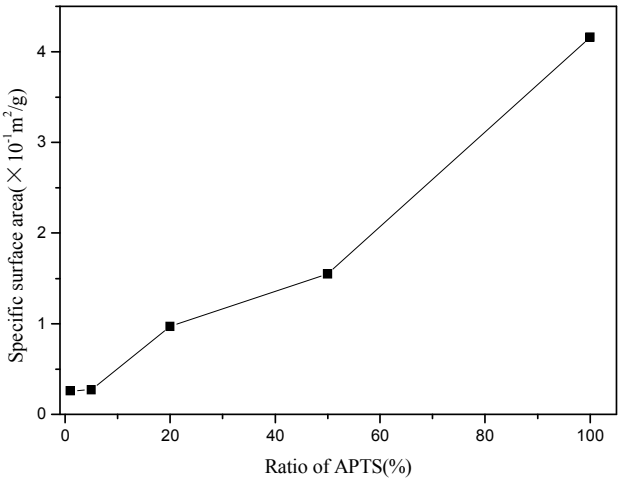


Figure 12 Specific surface areas of porous membranes

### 3.2.8 SEM measurement

SEM photographs of the polyphosphazene membranes were obtained under different conditions are shown in Figure 13. Picture a and b showed the cross section of membranes before the treatment by ammonia, picture c and d showed the membranes treated by ammonia, and picture c and d showed the composite membranes after the treatment of HF. It could be seen that before the treatment of HF, they are of the smooth surfaces. However, when the membranes are treated by ammonia, the surfaces became rougher. This suggested that under ammonia the 3-aminopropyltriethoxysilane hydrolysed to form silica, thus the surfaces became rougher. This phenomenon means that the polyphosphazene/silica composite membranes were formed. Furthermore, when the polyphosphazene/silica composite membranes were treated by HF, the silica dissolved, and the porous membranes were obtained accordingly. This phenomenon could be seen clearly in picture e and f.

RSC Advances Accepted Manuscript

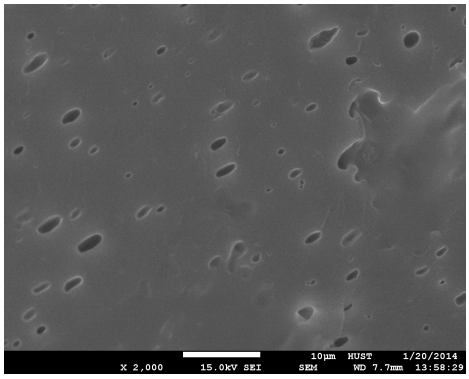


a

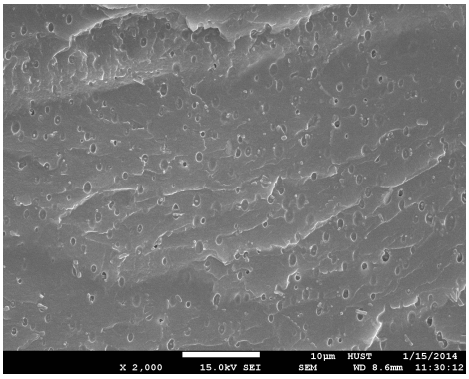


b

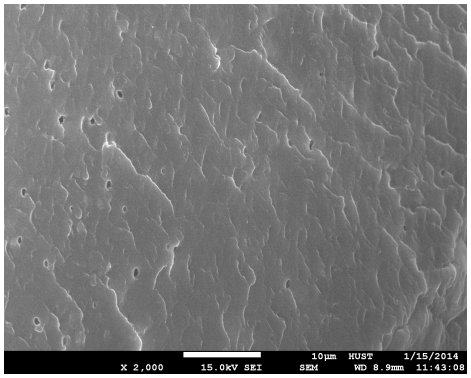


c

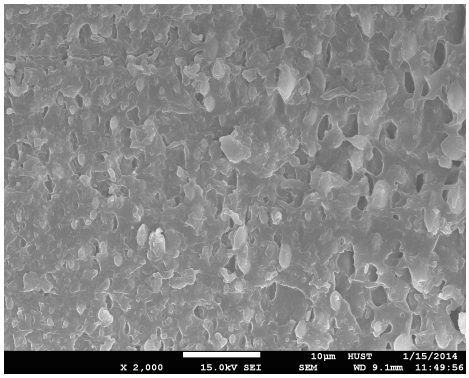


d

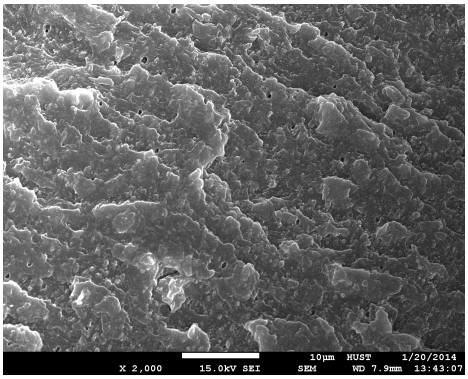


e

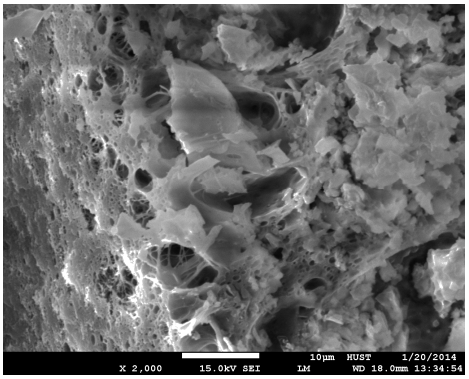


f

Figure 13 SEM of fracture surface of polyphosphaznenes

(a) PAB5 before being soaked in $NH_3 \cdot H_2O$, (b) PDA before being soaked in $NH_3 \cdot H_2O$, (c) Cross-linked composite PAB5, (d) Cross-linked composite PDA, (e) PAB5 etched by HF, (f) PDA corroded by HF.

RSC Advances Accepted Manuscript

**Conclusions:**

Polyphosphazene/silica composite membranes could be prepared through the hydrolysis of the 3-aminopropyltriethoxysilane side groups on polyphosphazenes. Moreover, the composite membranes could be treated by HF to dissolve the embeded silica, and finally the porous membranes could be obtained. The initial decomposition temperature increased when the formation of composite membranes occurred. In addition, the hydrophilicity could be tuned by introducing different side groups to the main chains of polyphosphazenes. Both the modulus and $T_g$ increased with the ratio of APTS. The as-prepared composite membranes and porous membranes could find their applications in membrane science and technology.

**Acknowledgments:**

The authors would like to thank the financial support of NSFC (41240026) and Scientific Research Foundation for the Returned Overseas Chinese Scholars, State Education Ministry.

RSC Advances Accepted Manuscript

**REFERENCES:**

[1] Allcock HR, Chemistry and applications of polyphosphazenes, Wiley: Hoboken, 2003.

[2] Weikel AL, Krogman NR, Nguyen NQ, Nair LS, Laurencin CT, Allcock HR. Polyphosphazenes that contain dipeptide side groups: synthesis, characterization, and sensitivity to hydrolysis. Macromolecules 2009; 42: 636-639.

[3] Orme CJ, Stewart FF. Mixed gas hydrogen sulfide permeability and separation using supported polyphosphazene membranes. J. Membr. Sci. 2005; 253: 243–249.

[4] Huang Y, Zhang P, Fu JW, Zhou YB, Huang XB, Tang XZ. Pervaporation of ethanol aqueous solution by polydimethylsiloxane/polyphosphazene nanotube nanocomposite membranes. J. Membr. Sci. 2009; 339: 85–92.

[5] Muldoona JG, Pintaurob PN, Wysickc RJ, Linc J, Ormed CJ, Stewart FF. Synthesis, characterization, and gas permeability of a series of 4-phenylphenoxy/phenoxy substituted polyphosphazene membranes. J. Membr. Sci. 2009; 334: 74–82.

[6] Houstona KS, Weinkaufa DH, Stewartb FF. Gas transport characteristics of plasma treated poly(dimethylsiloxane) and polyphosphazene membrane materials. J. Membr. Sci. 2002; 205: 103–112.

[7] Carriedo GA, Valenzuela ML, Valenzuela CD, Ushak S. Synthesis and pyrolysis of silicon and tin containing poly(2,2'-dioxy-1,1'-biphenoxy-phosphazenes). European Polymer Journal 2008; 44: 686–693.

RSC Advances Accepted Manuscript

[8] DeCollibus DP, Marin A, Andrianov AK. Effect of environmental factors on hydrolytic degradation of water-soluble polyphosphazene polyelectrolyte in aqueous solutions. Biomacromolecules 2010; **11**: 2033–2038.

[9] Greish YE, Benderb JD, Lakshmi S. Low temperature formation of hydroxyapatite-poly(alkyloxybenzoate)phosphazene composites for biomedieal applications. Biomaterials 2005; 26: l-9.

[10] Heyde M, Moens M, Vaeck LV, Shakesheff KM, Davies MC, Schacht EH. Synthesis and characterization of novel poly[(organo)phosphazenes] with cell-adhesive side groups. Biomacromolecules 2007; **8(5)**: 1436–1445.

[11] Ambrosio MA, Allcock HR, Katti DS, Laurencin CT. Biodegradable polycaprolactone–polyanhydrides blends. Biomaterials 2002; 23: 1667-1672.

[12] Andrianov AK, Chen JP, Payne LG. Preparation of hydrogel microspheres by coacervation of aqueous polyphosphazene solutions. Biomaterials 1998; 19: 109-115.

[13] Chun CJ, Lim HJ, Hong KY, Park KH, Song SC. The use of injectable, thermosensitive poly (organophosphazene)–RGD conjugates for the enhancement of mesenchymal stem cell osteogenic differentiation. Biomaterials 2009; 30: 6295-6308.

[14] Ren N, Huang XJ, Huang X, Qian YC, Wang C, Xu ZK. Controllable glycosylation of polyphosphazene via radical thiol–yne click chemistry. J. polym. sci. part A: polym. chem. 2012; 50: 3149–3157.

[15] Barrett EW, Phelps MVB, Silva RJ, Gaumond RP, Allcock HR. Patterning poly (organophosphazenes) for selective cell adhesion applications. Biomacromolecules 2005; 6: 1689-1697.

RSC Advances Accepted Manuscript

[16] Krogman NR, Weikel AL, Kristhart KA, Nukavarapu SP, Deng M, Nair LS, Laurencin CT, Allcock HR. The influence of side group modification in polyphosphazenes on hydrolysis and cell adhesion of blends with PLGA. Biomaterials 2009; 30: 3035-3041.

[17] Mal NK, Fujiwara M, Tanaka Y. Photocontrolled reversible release of guest molecules from coumarin-modified mesoporous silica. Nature 2003: 350–353.

[18] You YZ, Kalebaila KK, Brock SL, Oupicky D. Temperature-controlled uptake and release in PNIPAM-modified porous silica nanoparticles. Chem. Mater. 2008; 20, 3354-3359.

[19] Radu DR, Lai CY, Jeftinija K, Rowe EW, Jeftinija S, Lin VSY. A polyamidoamine dendrimer-capped mesoporous silica nanosphere-based gene transfection reagent. J. Am. Chem. Soc. 2004; 126: 13216–13217.

[20] Vallet-Regi M, Rámila A, del Real RP, Pérez-Pariente J. A new property of MCM-41: drug delivery system. Chem. Mater. 2001;13: 308–311.

[21] Slowing II, Trewyn BG, Lin VSY. Mesoporous silica nanoparticles for intracellular delivery of membrane-impermeable proteins. J. Am. Chem. Soc. 2007; 129: 8845–8849.

[22] He Q, Zhang Z, Gao Y, Shi J, Li Y. Intracellular Localization and Cytotoxicity of Spherical Mesoporous Silica Nano- and Microparticles. Small, 2009; 5: 2722–2729.

[23] Giraud I, Rapp M, Maurizis JC, Madelmont JC. Intracellular Localization and Cytotoxicity of Spherical Mesoporous Silica Nano- and Microparticles. J. Med. Chem. 2002; 45: 2116–2119.

RSC Advances Accepted Manuscript

[24] He QJ, Shi JL, Chen F, Zhu M, Zhang LX. Mesoporous silica nanoparticle based nano drug delivery systems: synthesis, controlled drug release and delivery, pharmacokinetics and biocompatibility. Biomaterials 2010; 31: 3335–3346.

[25] He Q, Zhang J, Shi J, Zhu Z, Zhang L, Bu W. The effect of PEGylation of mesoporous silica nanoparticles on nonspecific binding of serum proteins and cellular responses. Biomater 2010; 31: 1085-1092.

[26] Cheng XE, Liu SY, Shi WF. Synthesis and properties of silsesquioxane-based hybrid urethane acrylate applied to UV-curable flame-retardant coatings. Prog. org. coat. 2009: 1-9.

[27] Cheng XJ, Peng C, Zhang DH, Liu SZ, Zhang AQ, Huang H, Lian JS. A facile method for the preparation of thermally remendable cross-linked polyphosphazenes. J. Polym. Sci., PART A: Polym. Chem. 2013; 51: 1205-1214.

RSC Advances Accepted Manuscript